



# Sustainable Catalysis and Biomedical Applications: Advancing Iron-Based Oxygen Atom Transfer through Bioinspired Ligand Design



Ghassan Shannan, Zeina S. Malek, Nasser Thallaj

**Abstract:** This review analyses innovative semi-hemic bioinspired iron (III) complexes and their utility as catalysts for oxygen atom transfer (OAT) in both chemical and photochemical contexts. The research is motivated by the biological function of human endosulfatases (e.g., HSulf1 and HSulf2), enzymes that regulate heparan sulfate (HS) sulfation—a modification with profound roles in cancer, inflammation, and related pathologies. We detail the synthesis and characterization of novel dipyrin-supported iron complexes engineered to stabilize high-valent iron-oxo intermediates, which are critical reactive species in OAT catalysis. Emphasis is placed on employing green oxidants such as dioxygen and water to promote sustainable and efficient catalytic processes consistent with environmentally benign principles. Mechanistic insights into OAT pathways, elucidated through spectroscopic techniques, reveal detailed interactions between the iron centre and substrate molecules. A primary obstacle in the field—the instability of high-valent iron intermediates—is being addressed through innovative activation strategies that enhance both catalytic reactivity and complex stability. Additionally, the review summarises progress in developing endosulfatase inhibitors, particularly sulfamate-based agents, which offer promising avenues for modulating HS sulfation patterns. By elucidating fundamental iron-catalyzed mechanisms and refining the design of selective inhibitors, this work establishes a foundation for novel therapeutic approaches targeting diseases driven by aberrant HS activity. Future directions will focus on improving inhibitor potency and selectivity, as well as investigating targeted delivery methods. Together, these developments not only advance the fundamental understanding of iron-mediated oxidation chemistry but also forge new connections between glycochemistry and biomedical applications.

**Keywords:** Bioinspired; Iron (III) Complexes; Oxygen Atom Transfer (OAT); Catalysis; High-Valent Iron-Oxo Species; Sustainable Chemistry; Dipyrin.

## Nomenclature:

OAT: Oxygen Atom Transfer  
sMMO: Soluble Methane Monooxygenase  
EWGs: Electron-Withdrawing Groups  
OEC: Oxygen-Evolving Complex  
TON: Turn Over Number

TAMs: TetraAmido Macrocylic Ligands  
EXAFS: Extended X-Ray Absorption Fine Structure  
MS: Mass Spectrometry  
NMR: Nuclear Magnetic Resonance  
EPR: Electron Paramagnetic Resonance

## I. INTRODUCTION

This review focuses on the development of bioinspired iron complexes as catalysts for oxygen atom transfer (OAT) and hydroxylation reactions, consistent with green chemistry principles. Iron is an advantageous catalytic centre due to its natural abundance, low toxicity, and relevance to biological metalloenzymes [1]. Conventional methods for OAT and hydrogen atom abstraction often rely on precious or toxic metals and hazardous oxidants, presenting economic and environmental limitations that necessitate more sustainable alternatives [2].

Biological systems offer a paradigm for efficient oxidation, utilizing iron-dependent enzymes like cytochrome P450,  $\alpha$ -ketoglutarate-dependent hydroxylases, and soluble methane monooxygenase (sMMO) to perform selective transformations under mild conditions [3]. These enzymes operate through high-valent iron-oxo intermediates, which are highly effective at transferring oxygen atoms with precision [4]. For instance, cytochrome P450 activates a heme-bound iron to form a pivotal high-valent iron-oxo species (Compound I), enabling the hydroxylation of inert substrates such as cyclohexane [5].

Motivated by these natural catalysts, the design of biomimetic systems has emerged as a key research objective [6]. Synthetic metalloporphyrins, which replicate the heme cofactor's environment, have been extensively studied for OAT reactions, providing valuable mechanistic insights into iron-mediated oxidation [7]. A persistent challenge, however, is achieving the efficiency and selectivity of natural enzymes. This requires ligand architectures capable of stabilizing the reactive high-valent iron-oxo intermediates central to catalysis. Advances in ligand design, including the incorporation of electron-donating groups and novel scaffolds, aim to enhance catalyst stability and activity while enabling the use of green oxidants such as dioxygen or hydrogen peroxide.

The inherent instability of high-valent iron-oxo species poses a significant obstacle to their characterisation and application. Sophisticated spectroscopic techniques—such as Mössbauer, EPR, and resonance Raman spectroscopy—is essential for probing the electronic structure and

Manuscript received on 16 December 2025 | Revised Manuscript received on 07 January 2026 | Manuscript Accepted on 15 February 2026 | Manuscript published on 28 February 2026.

\*Correspondence Author(s)

**Prof. (Dr.) Ghassan Shannan**, Department of Biochemistry, Arab International University, Damascus, Syria. Email ID: [gshannan@aiu.edu.sy](mailto:gshannan@aiu.edu.sy), ORCID ID: [0009-0005-9673-8564](https://orcid.org/0009-0005-9673-8564)

**Prof. (Dr.) Zeina S. Malek**, Department of Physiology, Arab International University, Damascus, Syria. Email ID: [z-malek@aiu.edu.sy](mailto:z-malek@aiu.edu.sy), ORCID ID: [0009-0006-7075-7991](https://orcid.org/0009-0006-7075-7991)

**Prof. (Dr.) Nasser Thallaj\***, Department of Pharmaceutical Chemistry and Drug Quality Control, Arab International University, Damascus, Syria. Email ID: [profthallaj@gmail.com](mailto:profthallaj@gmail.com), ORCID ID: [0000-0002-6279-768X](https://orcid.org/0000-0002-6279-768X)

© The Authors. Published by Lattice Science Publication (LSP). This is an open-access article under the CC-BY-NC-ND license <https://creativecommons.org/licenses/by-nc-nd/4.0/>

# Sustainable Catalysis and Biomedical Applications: Advancing Iron-Based Oxygen Atom Transfer Through Bioinspired Ligand Design

reactivity of these transient intermediates [8].

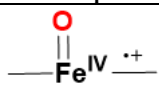
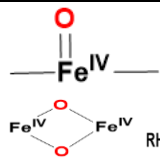
The current work details the synthesis and investigation of novel iron complexes, building upon innovations in ligand design [9]. Particular emphasis is placed on dipyrin-based ligand platforms, which offer a promising strategy for stabilizing reactive iron-oxo species and advancing iron-catalysed oxidation [10]. Ultimately, the development of such bioinspired catalysts represents a strategic step toward sustainable chemical synthesis. By merging insights from biological catalysis with synthetic chemistry, this research aims to contribute to the foundation of efficient and environmentally responsible catalytic systems, addressing

enduring challenges in chemical synthesis and expanding fundamental knowledge of iron-mediated processes [11].

## A. Enzymatic Systems Facilitating Oxidation in Nature

Two major classes of enzymatic systems chiefly drive biological oxidation. The first category consists of heme-dependent proteins, such as cytochrome P450 enzymes. The second category encompasses non-heme iron enzymes, including soluble methane monooxygenases and  $\alpha$ -ketoglutarate-dependent hydroxylases (Table 1).

**Table I: Selection of Metalloenzymes Involved in Biological Oxidation**

Catalytic Metalloenzyme	Active Species	Catalytic Reaction
Cytochrome P450	 $\text{C-C/C-H} + \text{O}_2 \xrightarrow[2e^-]{2\text{H}^+} \text{C-C/C-OH} + \text{H}_2\text{O}$	
$\alpha$ -ketoglutarate-dependent hydroxylases. Soluble methane monooxygenases	 $\text{RH} + \text{R}'\text{COCO}^-\text{OH} + \text{O}_2 \rightarrow \text{ROH} + \text{R}'\text{C}'\text{OOH} + \text{CO}_2$	$\text{CH}_4 + \text{O}_2 \xrightarrow[2e^-]{2\text{H}^+} \text{CH}_3\text{OH} + \text{H}_2\text{O}$

## B. Cytochrome P-450

Cytochrome P-450 enzymes constitute a widespread family of heme-containing metalloenzymes that serve as highly versatile monooxygenases in biological systems. They are distinguished by their capacity to activate dioxygen and catalyze the insertion of a single oxygen atom into a diverse array of organic substrates under mild physiological conditions. Their catalytic functions include aliphatic hydroxylation, aromatic oxidation, epoxidation, and sulfoxidation, utilizing NADPH as the requisite electron donor. A feature of particular interest to chemists is their ability to perform selective hydroxylation of inert compounds, such as cyclohexane, while preserving enzymatic integrity [12].

This reactivity is derived from a uniquely structured active site centred on an iron protoporphyrin IX cofactor (Figure 1). The iron centre is axially coordinated by a conserved cysteine residue, whose thiolate ligand is essential for catalytic activity. The opposite axial coordination site is variable, often occupied by water or the substrate, thereby creating an environment optimised for the binding and activation of dioxygen [13].

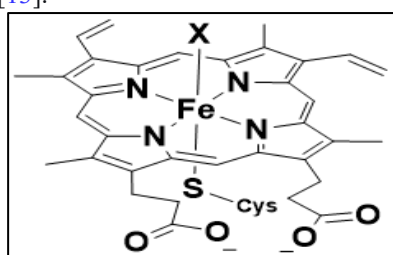


**[Fig.1: Iron Protoporphyrin IX Active Site of Cytochromes P-450s, X: Labile Ligand]**

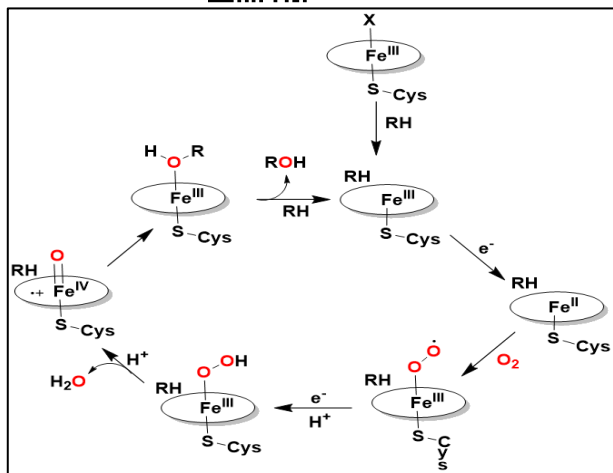
## C. Mechanism of Cytochrome P-450

The catalytic cycle of cytochrome P-450 is presented in Scheme I-1. The process begins with substrate binding to the enzyme's active site, displacing a loosely coordinated ligand and frequently inducing a change in the iron centre's spin state. Subsequently, the iron core is reduced from the Fe(III) to the Fe(II) state by NADPH, enabling the binding of molecular oxygen. A further one-electron reduction and protonation step then yields a crucial Fe(III)-hydroperoxo intermediate [14].

This hydroperoxo species undergoes O–O bond heterolysis following an additional protonation event, generating the pivotal high-valent oxidant: an iron(IV)-oxo species (ferryl) coupled with a porphyrin  $\pi$ -cation radical, known as Compound I. This highly reactive intermediate has been spectroscopically characterized in various heme systems. Its identity is confirmed by Mössbauer parameters ( $\delta = 0.05$ – $0.14$  mm/s;  $\Delta E_Q = 0.90$ – $1.33$  mm/s), indicative of a low-spin  $S=1$  Fe(IV) center; by EPR signals around  $g \approx 2$ , which are characteristic of a radical species; and by resonance Raman spectroscopy showing a distinctive Fe–O vibrational band in the  $750$ – $790$   $\text{cm}^{-1}$  range [15].

The final step involves the transfer of an oxygen atom from Compound I to the bound substrate, thereby producing the oxidised product. Although theoretical studies suggest some delocalization of the radical character to the axial thiolate ligand or surrounding protein residues, spectroscopic data conclusively establish the iron(IV)-oxo porphyrin  $\pi$ -cation radical as the primary species responsible for the broad oxidative catalysis performed by cytochrome P-450 enzymes (Scheme 1).





**Scheme 1: Catalytic Cycle for Oxygen Activation and Transfer by Cytochrome P-450s.**

**D.  $\alpha$ -Ketoglutarate-Dependent Hydroxylases**

A distinct and diverse family of mononuclear non-heme iron enzymes, the Iron (II) and  $\alpha$ -ketoglutarate-dependent hydroxylases, catalyze a wide spectrum of hydroxylation reactions. In these processes,  $\alpha$ -ketoglutarate ( $\alpha$ -KG) functions as an essential co-substrate. Structurally, the active site of these enzymes features a single iron(II) centre coordinated within a protein-derived ligand field. This field typically consists of three endogenous amino acid residues—often two histidines and one aspartate or glutamate—arranged in a facial triad, along with three water-derived ligands in the resting state (Figure 2).

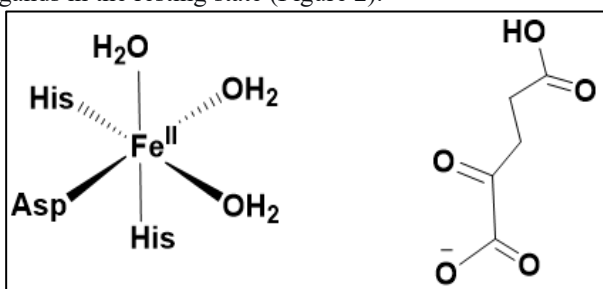


**[Fig.2: Active Site of  $\alpha$ -Ketoglutarate-Dependent Hydroxylases (Left) and  $\alpha$ -Ketoglutarate (Right)]**

The oxidative decarboxylation of  $\alpha$ -ketoglutarate serves to activate dioxygen, producing a highly reactive iron (IV)-oxo (ferryl) intermediate. This potent oxidizing species facilitates the hydroxylation of a broad array of substrates, including methylated nucleotides and lipids [16].

The accepted mechanistic framework for this catalysis, corroborated by spectroscopic investigations of enzymes such as Clavaminate Synthase 2 and Taurine Dioxygenase, was definitively established in 2003. A pivotal study by Bollinger and Krebs utilized Mössbauer spectroscopy to confirm the formation of a high-spin ( $S = 2$ ) non-heme iron (IV)-oxo intermediate within the Taurine Dioxygenase catalytic cycle [17].

Distinct spectroscopic signatures characterized this high-valent iron species. Mössbauer spectroscopy identified it through an isomer shift ( $\delta$ ) of 0.31 mm/s and a quadrupole splitting ( $\Delta E_Q$ ) of 0.88 mm/s. Concurrently, resonance Raman spectroscopy detected an Fe–O stretching vibration at 821  $\text{cm}^{-1}$ , which exhibited the expected isotopic shift to 787  $\text{cm}^{-1}$  upon substitution with  $^{18}\text{O}$  (Figure 3).

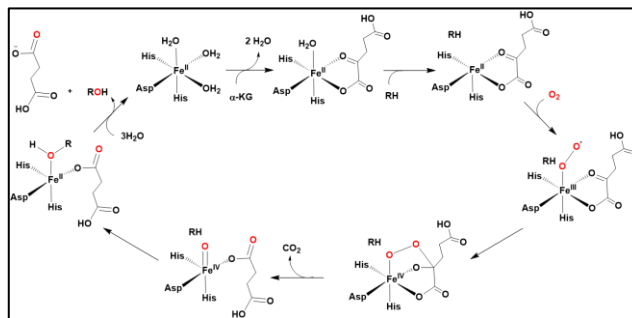


**[Fig.3: Proposed Mechanism of Catalytic Cycle for  $\alpha$ -Ketoglutarate-Dependent Hydroxylases]**

**E. Soluble Methane Monooxygenases**

Soluble methane monooxygenases (sMMOs) are bacterial enzymes that possess a crucial functional similarity to both cytochrome P-450s and  $\alpha$ -ketoglutarate-dependent hydroxylases: the capacity to hydroxylate the remarkably strong C–H bond of methane ( $\text{BDE} \approx 105 \text{ kcal/mol}$ ). Consistent with these other systems, sMMOs utilize dioxygen as the oxidant and NAD(P)H as the electron donor. A distinguishing structural characteristic of sMMOs, however, is their dinuclear non-heme iron active site (Figure 4).

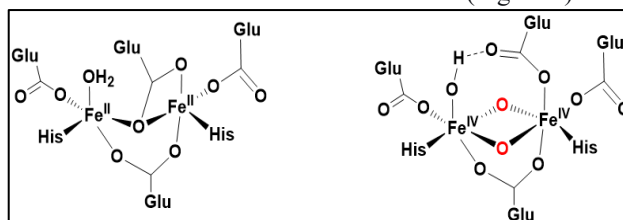


**[Fig.4: Dinuclear Iron Active Site in sMMO : (Left) Reduced Form, (Right) Oxidized Form]**

In contrast to mononuclear iron enzymes, the catalytically active species in sMMO is a bis- $\mu$ -oxo diiron(IV) complex, frequently characterized as possessing a "diamond core" structure. This pivotal intermediate has been spectroscopically characterized, defining its key properties. The catalytic cycle initiates with dioxygen activation at the reduced diiron(II) centre, generating a peroxo-bridged diiron(III) intermediate. Subsequent homolytic O–O Bond cleavage yields the highly reactive bis- $\mu$ -oxo diiron(IV) species, which is capable of oxidising methane (Figure 5).

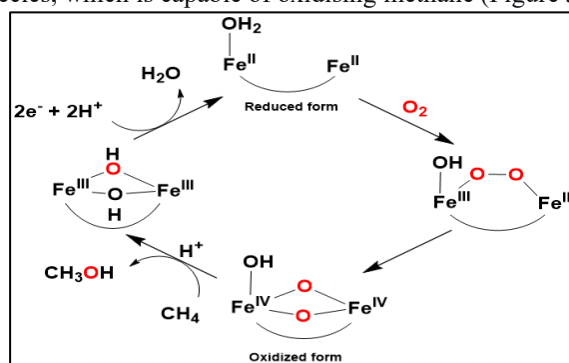


**[Fig.5: Proposed Mechanism for Methanol Conversion Using sMMO]**

Biological systems utilize metalloenzymes to achieve hydrocarbon oxygenation under ambient conditions. This process is driven by the



# Sustainable Catalysis and Biomedical Applications: Advancing Iron-Based Oxygen Atom Transfer Through Bioinspired Ligand Design

activation of dioxygen to generate high-valent iron-oxo intermediates, facilitated by biological reductants such as NAD(P)H or by co-substrates such as  $\alpha$ -ketoglutarate. While these natural catalysts exhibit exceptional efficiency and selectivity, their practical utility is constrained by challenges in isolation and large-scale production; for instance, the genetic sequences encoding cytochrome P-450 enzymes were identified only in recent decades. These limitations highlight the critical need to develop durable synthetic analogues that can replicate enzymatic functions. Investigating such biomimetic systems not only provides a viable practical alternative but also enhances fundamental mechanistic insights into natural catalytic processes [18].

## F. Synthetic Iron Catalysts for Oxidation Reaction

Following the selection of a central metal ion, chemists must refine the two primary determinants of catalytic performance: the ligand framework and the activation protocol. The ligand architecture is essential for modulating the metal's electronic properties and steric environment, which in turn dictates the pathway for catalyst activation. The synergistic relationship between these two elements is examined in the following section [19].

## II. LIGAND DESIGN

Substantial research is currently focused on creating efficient synthetic analogues of metalloenzymes for catalytic oxidation reactions. Given that the protein scaffold and its endogenous ligands are fundamental to enzymatic activity, synthetic chemists frequently design ligand architectures grounded in biological motifs. These designed ligands are generally classified into two distinct categories—biomimetic and bioinspired—based on their underlying design strategy [20].

### A. Biomimetic Approach

The development of synthetic catalysts that emulate the oxidative capabilities of metalloenzymes is a dynamic and central pursuit in contemporary chemistry. The extraordinary efficiency of these biological catalysts is largely attributed to the specific protein-derived ligand environment that encapsulates the metal ion [21]. Consistent with this concept, the design of synthetic catalysts frequently employs ligand systems classified as either biomimetic or bioinspired. A biomimetic ligand is a synthetic construct engineered to closely reproduce the spectroscopic characteristics and coordination geometry of a native enzymatic cofactor [22]. A classic illustration is the porphyrin macrocycle, which mimics the structure of protoporphyrin IX found in cytochrome P-450, thereby providing a tetradentate, nitrogen-rich coordination sphere analogous to the heme centre (Figure 6).

The utilization of metalloporphyrins as oxidation catalysts has grown substantially since the foundational work of Groves and coworkers in 1979, which demonstrated that chloro-5,10,15,20-tetraphenylporphyriniron (III) ( $\text{Fe}^{\text{III}}\text{TPPCl}$ ) could catalyze alkene epoxidation and alkane hydroxylation using iodobenzene as a terminal oxidant. Subsequent advances have yielded successive generations of metalloporphyrins with strategic modifications at the *meso* and  $\beta$ -pyrrolic positions. These tailored porphyrin derivatives have demonstrated markedly enhanced catalytic efficiency across a range of oxidation reactions (Figure 6).

The influence of these peripheral substituents on modulating catalyst reactivity will be analyzed in the subsequent section [23].

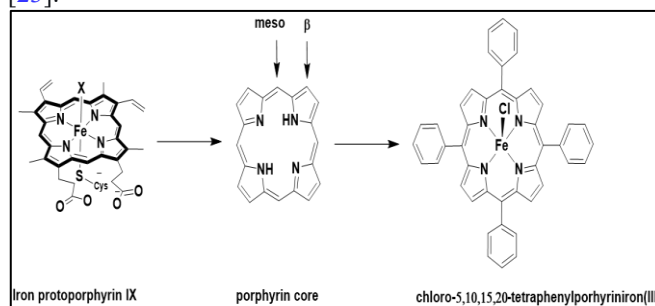


**[Fig.6: Porphyrin Core Used for Synthetic Porphyrin Ligand and Formula of Metalloporphyrin of the First Generation Used in the Model System of Cytochrome P450S]**

A characteristic and functionally essential element of cytochrome P-450 enzymes is an axial thiolate ligand that substantially boosts the catalytic activity of the heme iron [24]. To synthetically probe this influence, chemists have engineered model complexes in which a thiolate ( $\text{RS}^-$ ) group is integrated into the porphyrin's ligand environment. A widely adopted tactic to prevent undesirable ligand exchange in solution is to covalently link the thiolate donor to the porphyrin skeleton using a "S-bridge" or "S-tail" tether [25]. The pioneering iron porphyrin complex featuring a coordinated alkylthiolate anion for oxidation catalysis was documented in 1990 [26]. This work established that the thiolate ligand could accelerate the oxidation of substrates such as 2,4,6-tri-*tert*-butylphenol by nearly two orders of magnitude relative to the conventional  $\text{Fe}^{\text{III}}\text{TPPCl}$  catalyst when employing alkyl hydroperoxides as oxidants [27].

The suggested catalytic sequence commences with the formation of an alkyl peroxide adduct at the iron porphyrin centre, succeeded by heterolytic O–O bond cleavage to produce a high-valent iron-oxo species [28]. This potent oxidant subsequently reacts with the substrate to deliver the oxygenated product. The pronounced rate acceleration is principally attributed to the robust electron-donating capacity of the thiolate ligand, which lowers the activation barrier for O–O bond scission and stabilizes the resulting iron-oxo intermediate [29]. Corroborative evidence for this electron-donating effect comes from cyclic voltammetry, which reveals a significant cathodic shift of approximately 200 mV in the  $\text{Fe}^{\text{III}}/\text{Fe}^{\text{II}}$  redox potential for the thiolate-bound complex compared to  $\text{Fe}^{\text{III}}\text{TPPCl}$  (Figure 7).

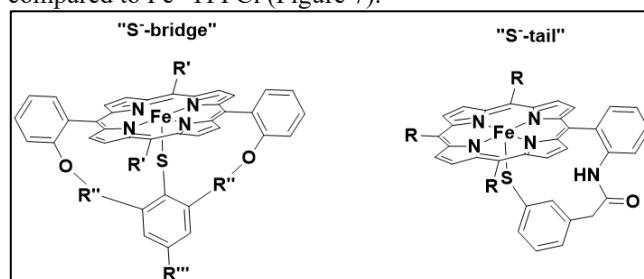


**[Fig.7 : Synthetic Metalloporphyrins Containing a « S-bridge » Ligand (left) and « S-tail » Ligand (right)]**

While the research by Hirobe's Although group-produced catalytic outcomes were encouraging, their intrinsic instability substantially





hampered the development of synthetic heme metalloporphyrins bearing axial thiolate ligands [30]. The thiolate moiety is susceptible to oxidation, resulting in irreversible disulfide bond formation. This strong electron-donating character consequently renders the complexes unstable under the highly oxidative conditions required for catalysis, ultimately precluding further investigation of this strategy [31].

In an alternative design approach, the incorporation of electron-withdrawing groups (EWGs) at the *meso* or  $\beta$  positions of the porphyrin macrocycle has been more successful. As summarized in Table 2 and Figure 8, this structural modification enhances catalytic efficiency in reactions such as cyclohexene oxidation. EWGs increase the electrophilicity of the critical iron-oxo ( $\text{Fe}=\text{O}$ ) intermediate, thereby augmenting its reactivity toward electron-rich substrates like alkenes. A concurrent advantage is that this electronic tuning also enhances the catalyst's resistance to oxidative degradation, thereby improving operational stability [32].

**Table II: Cyclohexene Epoxidation by PhIO Catalysed by Iron Porphyrin Complex**

Catalysts	Substrate	Product	TON
FeIII(TPP) Cl	cyclooctene	Cyclooctene	32
FeIII(TDCPP) Cl		epoxyde	72
FeIII( $\beta$ -F8TPP) Cl			81

**B. Cyclohexene/PhIO/Catalyst = 100/100/1, Solvent: DCM. TON Based on PhIO in 2h**

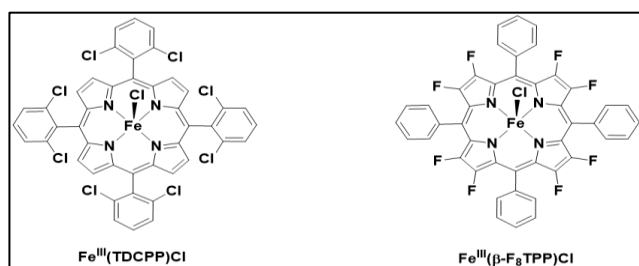


**[Fig.8: Structure of Iron (III) Porphyrins with an Electron-Withdrawing Group in the Meso and  $\alpha$  Positions]**

The past two decades have witnessed significant advancements in the design of biomimetic non-heme iron complexes capable of generating iron-oxo species for catalytic oxidation [33]. A notable contribution in 2003 was a synthetic model for  $\alpha$ -ketoglutarate-dependent hydroxylases that employed a tridentate  $\text{Tp}^{\text{Ph}_2}$  (hydrotris(3,5-diphenylpyrazol-1-yl) borate) ligand to mimic the native enzyme's facial triad coordination environment [34]. In this system, an  $\alpha$ -keto acid functions as a sacrificial two-electron donor, providing the electrons necessary for  $\text{O}_2$  activation. This non-heme model complex successfully activated dioxygen via oxidative decarboxylation and demonstrated broad catalytic activity, including sulfide oxidation, cis-dihydroxylation of alkenes, and hydroxylation of alkanes. A key finding was the observation of intramolecular hydroxylation of a phenyl substituent on the  $\text{Tp}^{\text{Ph}_2}$  ligand in the absence of an external substrate, a reaction ascribed to the group's proximity to the metal centre [35]. However, despite these functional demonstrations, direct spectroscopic identification or isolation of the proposed reactive

intermediates in these transformations was not achieved (Figure 9).

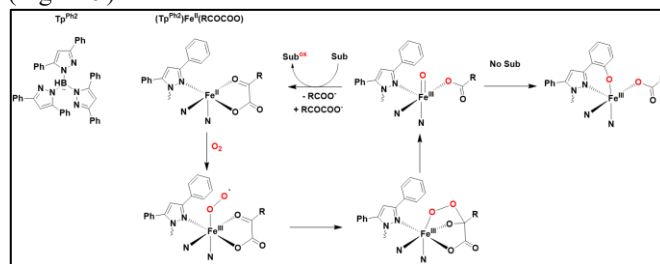


**[Fig.9: Synthetic Model for  $\alpha$ -Ketoglutarate-Dependent Iron Enzymes]**

The biomimetic design strategy centres on replicating the structural motifs of natural enzymes to develop synthetic catalysts for the oxidation of alkanes and alkenes [36]. Although such catalysts frequently display only moderate reactivity—often constrained by their inherent instability under oxidative conditions—they function as essential molecular probes for deciphering the mechanistic principles of native metalloenzymes [37]. Reconstructing only isolated components of the enzymatic architecture, absent the full complexity of the protein environment, invariably alters the properties of the active site. Nevertheless, studies of these biomimetic systems are vital for pinpointing the fundamental features responsible for the exceptional efficiency of biological catalysis. This knowledge, in turn, guides the rational design of more sophisticated, bioinspired oxidation catalysts [38].

### III. BIOINSPIRED APPROACH

In contrast to the biomimetic approach, the bioinspired strategy aims to identify and apply the fundamental chemical principles underlying biological function [39]. A pivotal concept in iron enzyme catalysis is the generation of a transient high-valent iron-oxo intermediate, which is stabilized within the sophisticated protein environment [40]. To synthetically emulate this stabilisation, researchers use ligands with multiple nitrogen or oxygen donor atoms, which create a strongly electron-donating coordination sphere capable of supporting these highly oxidised states [41].

A prime illustration of a bioinspired ligand is the tetradentate Salen framework, which chelates a metal ion via two phenolic oxygen and two imine nitrogen atoms. This coordination geometry leaves two axial sites open for interaction with oxidants and substrates. Similar to porphyrins, these dianionic ligands are exceptionally proficient at stabilising high-valent metal centres. A principal benefit of the Salen platform is its synthetic modularity; methodical alteration of its substituents has yielded successive catalyst generations with enhanced reactivity and durability. The ligand's rigid, planar tetradentate structure can accommodate various metal ions, including manganese, iron, and ruthenium [42]. A seminal accomplishment in this area is Jacobsen's catalyst—a chiral manganese–Salen complex that catalyzes the asymmetric epoxidation of alkenes. This catalyst is used industrially in the synthesis of Indinavir, an HIV protease inhibitor, underscoring the substantial



# Sustainable Catalysis and Biomedical Applications: Advancing Iron-Based Oxygen Atom Transfer Through Bioinspired Ligand Design

practical utility achievable through bioinspired catalytic design (Figure 10).

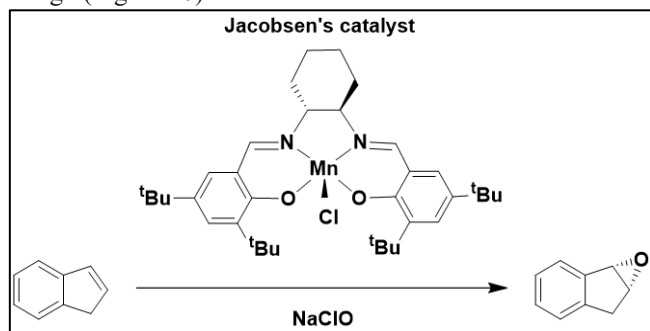


**[Fig.10: Jacobsen's Catalyst Used for Asymmetric Epoxidation in the Industrial Synthesis of Indinavir]**

Advancing from fundamental scaffolds such as Salen and Margerum's macrocyclic tetraamines, TetraAmido Macrocyclic Ligands (TAMLs) represent a major ligand class refined over four decades, largely through the research of Collins, Gupta, and their associates. These tetraanionic ligands create a potent electron-donating environment, highly proficient at stabilizing metal centres in high oxidation states [43].

A defining characteristic of the TAML framework is its geometrically rigid macrocyclic core, which provides exceptional stability by inhibiting intramolecular rearrangements that commonly result in catalyst decomposition. Through seven iterative design generations, fifth-generation TAML systems have formed an iron(V)-oxo species, [(bTAML)Fe<sup>V</sup>=O]<sup>1-</sup>, under ambient conditions [44]. This high-valent intermediate exhibits substantial reactivity, capable of cleaving the strong C–H bonds of cyclohexane with high selectivity and remarkable catalytic durability (Figure 11).

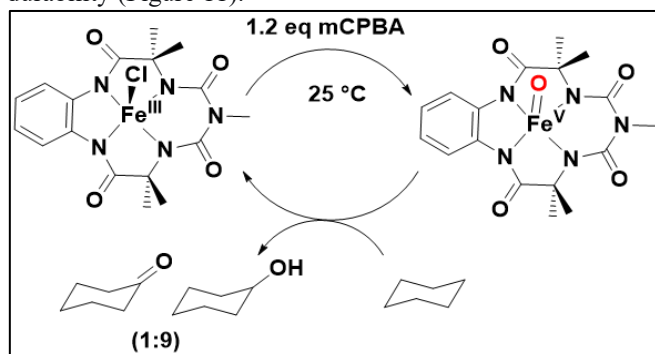


**[Fig.11: Operationally Stable, Highly Active Iron(V)-Oxo Supported by b-TAML and Their Reactivity Toward Cyclohexane Oxidation]**

The formation of high-valent metal-oxo species is not exclusive to anionic ligand systems. An alternative strategy employs synthetic, neutral polynitrogen ligands inspired by biological donors such as histidine. Since the late 1980s, a diverse range of such ligand architectures has been developed to produce reactive metal-oxo intermediates for catalytic oxidation [45].

These polydentate ligands often integrate  $\pi$ -accepting nitrogen donors—such as pyridine, benzimidazole, or imidazole—with  $\sigma$ -donating tertiary amines. Their inherent conformational flexibility allows them to adapt to the geometric requirements of various metal ions. While the

absence of a formal negative charge can reduce the stability of the resulting high-valent metal-oxo complex, it can concurrently produce a more powerful oxidant by diminishing electron density at the metal centre [46].

A prominent example reported in 2011 featured a nonheme iron (IV)-oxo species stabilized by the Me<sub>3</sub>NTB ligand, which proved competent for alkane C–H bond activation and thioanisole sulfoxidation [47]. This complex was notable as the first synthetic nonheme iron-oxo species to exceed the reactivity of the benchmark iron(IV)-oxo porphyrin  $\pi$ -cation radical, (Por<sup>+</sup>•)Fe<sup>IV</sup>=O. The synthetic accessibility and tunability of polynitrogen ligands have been instrumental in enhancing the reactivity of such systems [48]. This advancement was further highlighted in 2015 with the report of an Fe<sup>V</sup>=O species supported by a PyNMe<sub>3</sub> macrocyclic ligand, which demonstrated unparalleled activity for cyclohexane hydroxylation, outperforming all previously documented iron-oxo catalysts (Figure 12).

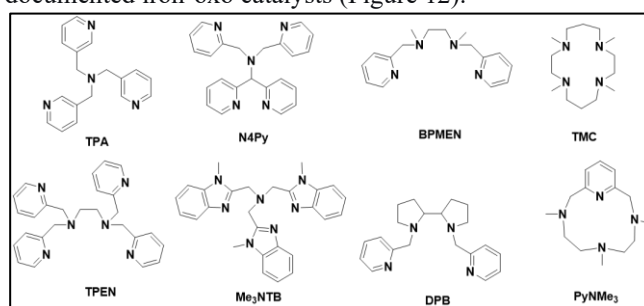


**[Fig.12: Examples of Poly-Nitrogen Neutral Ligands]**

Investigations have demonstrated that altering the axial ligand within TMC-based complexes offers a straightforward strategy for modulating the electrophilicity of iron-oxo species, thus regulating their reactivity in oxygen atom transfer (OAT) processes.[47] As the OAT mechanism involves a two-electron transfer from the substrate to the iron core, the electrophilic character of the iron-oxo moiety is a pivotal factor governing reaction kinetics. This property can be experimentally quantified by determining the reduction potential of the Fe<sup>n</sup>=O/Fe<sup>n-1</sup>=O redox couple. A more pronounced electrophilic nature, as indicated by a higher potential, directly corresponds to increased OAT activity, as evidenced in Figure 13.

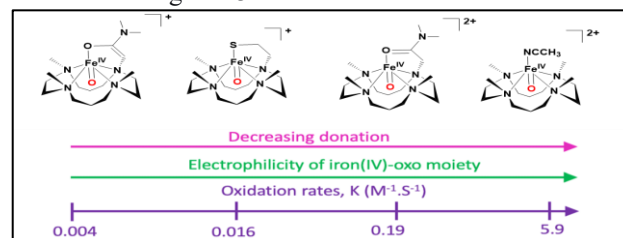


**[Fig.13: OAT Reactivity in PPh<sub>3</sub> Oxidation by a Series of Iron (IV)-Oxo Complexes]**

## A. Activation Strategies and Mechanistic Insights

### i. Using Chemical Oxygen Donor Agents

The past decade has seen the successful synthesis of a diverse array of synthetic high-valent iron-oxo complexes utilizing various ligand platforms and preparation





methods. A prevalent synthetic approach involves the oxidation of an iron complex precursor with oxygen-atom-donor reagents such as iodosylbenzene, sodium hypochlorite, peracids, and hydroperoxides. In particular, two-electron oxidants like iodosylbenzene, NaOCl, and *m*-CPBA can directly convert iron(II) precursors into iron(IV)-oxo species, or oxidize iron(III) precursors to generate iron(V)-oxo or iron(IV)-oxo ligand radical cations [48]. The general mechanism for this transformation is proposed to occur in two primary steps: initial adduct formation between the oxidant and the iron centre, followed by oxygen atom transfer initiated by heterolytic cleavage of the O–X bond (Figure 14).

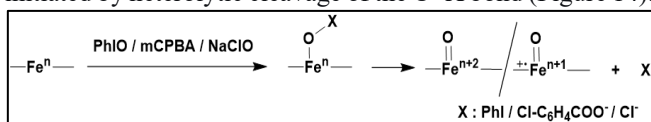


[Fig.14: Proposed Mechanism for the Iron-Oxo Species Formation Using a Two-Electron Oxidant]

Extensive mechanistic studies have employed hydrogen peroxide as an oxidant to probe the pathways of O–O bond activation in biomimetic systems. When an iron(II) precursor is treated with excess hydrogen peroxide in acetonitrile, it is proposed to be oxidized by 0.5 equivalents of H<sub>2</sub>O<sub>2</sub> to generate an iron(III) complex [49]. This iron(III) species then reacts rapidly with an additional equivalent of hydrogen peroxide to form a hydroperoxo iron(III) intermediate. The heterolytic cleavage of the O–O bond within this intermediate subsequently produces an iron(V)-oxo species. Therefore, the net conversion of an iron(III) precursor to an iron(V)-oxo complex requires the consumption of only one equivalent of hydrogen peroxide, as depicted in Figure 15.

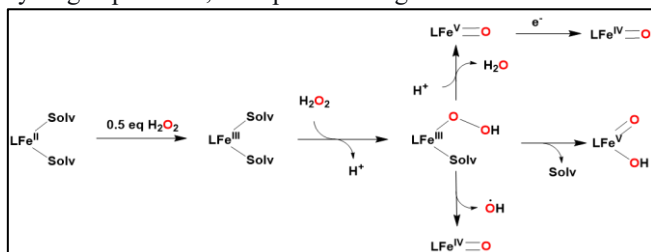


[Fig.15 : Proposed Mechanism for Generation of an Iron(V)-Oxo Species From Iron (II) Precursor Using H<sub>2</sub>O<sub>2</sub>]

In 2011, researchers successfully characterized the [(Fe<sup>V</sup>=O) TMC]<sup>2+</sup> species, generated by reacting [Fe<sup>II</sup>(TMC)]<sup>2+</sup> with excess hydrogen peroxide under acidic conditions. The formation kinetics of this iron(IV)-oxo complex exhibited proton-dependence, supporting a mechanism wherein proton-assisted heterolytic cleavage of the O–O bond in an Fe<sup>III</sup>–OOH intermediate initially yields a transient [(Fe<sup>V</sup>=O) TMC]<sup>3+</sup> species. This iron(V)-oxo intermediate is then rapidly reduced by one electron to produce the final iron(IV) product [50].

Although homolytic cleavage of the Fe<sup>III</sup>–OOH intermediate represents a conceivable alternative route to an iron(IV)-oxo species, density functional theory (DFT) calculations indicate this pathway is thermodynamically unfavourable [51].

In a separate base-promoted pathway, investigations have demonstrated that the stoichiometric reaction of [Fe<sup>II</sup>(TMC)]<sup>2+</sup> and [Fe<sup>II</sup>(TMC-py)]<sup>2+</sup> with hydrogen peroxide yields the corresponding Fe<sup>V</sup>=O species in approximately 90% yield. This high efficiency, achieved using only one

equivalent of H<sub>2</sub>O<sub>2</sub>, suggests a mechanism involving an iron(II) peroxo precursor that undergoes heterolytic O–O bond scission [52]. However, the proposed iron(II) peroxo intermediate remains hypothetical, as the iron(II) starting material could alternatively be oxidized via single-electron transfer from hydrogen peroxide, generating an iron(III) complex directly (Figure 16).

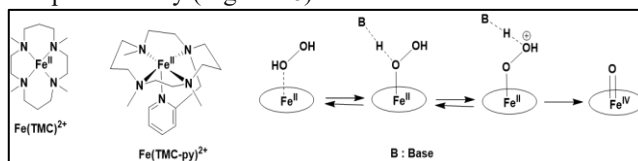


[Fig.16: Proposed Mechanism for the Base-Catalyzed Formation of Iron (IV)-oxo From Iron (II) Precursor and H<sub>2</sub>O<sub>2</sub>]

ii. Using dioxygen as an oxygen atom source

The controlled application of chemical oxidants facilitates the generation and detailed study of reactive iron intermediates, thereby enabling the characterisation of these often-transient species and the elucidation of their reaction pathways [53]. From an environmental standpoint, however, the utilization of green oxygen sources is a key objective. Dioxygen emerges as an ideal candidate due to its natural abundance, sustainability, and role as the terminal oxidant in numerous biological oxidation reactions catalyzed by both heme and non-heme iron enzymes [54].

Inspired by cytochrome P-450 enzymes, synthetic iron complexes can also activate dioxygen to form iron-oxo species when supplied with a proton source and a sacrificial electron donor such as BNAH, cobaltocene, or BH<sub>4</sub><sup>–</sup> [55]. A representative demonstration of this strategy was reported by Banse and colleagues using the [Fe<sup>II</sup>(TMC-py)]<sup>2+</sup> complex with BPh<sub>4</sub><sup>–</sup> as the reductant and HClO<sub>4</sub> as the proton source. In this system, dioxygen undergoes reductive activation at the iron (II) centre, proceeding via an iron(III)-superoxo intermediate that is subsequently protonated to form an Fe<sup>III</sup>–OOH species. This hydroperoxo complex then undergoes O–O bond cleavage to yield the final iron (IV)-oxo product (Figure 17).

The scission of the O–O bond may proceed through homolytic or heterolytic pathways, with the resulting fragments rapidly collapsing to produce the iron (IV)-oxo species—a process mechanistically similar to that observed with hydrogen peroxide under acidic conditions [56]. In this study, the resulting [Fe<sup>IV</sup>=O(TMC-py)]<sup>2+</sup> complex was fully characterized using multiple spectroscopic techniques, including conclusive identification by single-crystal X-ray diffraction [129].

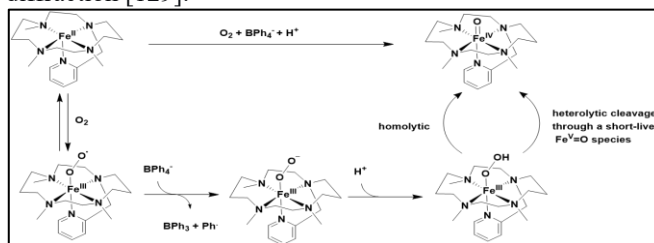


[Fig.17: Proposed Dioxygen Activation Mechanism Using [Fe<sup>II</sup>(TMC-Py)]<sub>2</sub><sup>+</sup>]

The concept of electrochemically activating dioxygen was originally proposed in prior studies. A significant 2013



# Sustainable Catalysis and Biomedical Applications: Advancing Iron-Based Oxygen Atom Transfer Through Bioinspired Ligand Design

investigation by Dey and co-workers examined this process using an iron(III) porphyrin and integrated electrolysis with resonance Raman spectroscopy [57]. By employing  $^{18}\text{O}$ -labeled dioxygen, this methodology enabled the direct observation of critical intermediates—specifically an iron(III) peroxy species and an iron(IV)-oxo complex—generated during the electrochemical reduction of the  $\text{Fe}^{\text{II}}\text{-O}_2$  adduct at a potential of  $-0.5\text{ V}$  versus  $\text{Ag}/\text{AgCl}$  [130].

However, their findings warrant a detailed assessment. The study reported an  $\text{Fe-O}$  stretching frequency of  $780\text{ cm}^{-1}$  for the iron(IV)-oxo species. This observation is significant, as the  $\text{Fe-O}$  vibrations for all other documented heme and non-heme iron-oxo intermediates consistently fall within the  $800\text{--}850\text{ cm}^{-1}$  range [58]. This discrepancy will be analyzed in the following section (Figure 18).

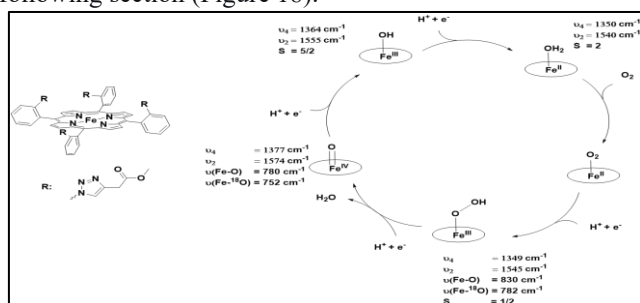


**[Fig.18: Proposed Mechanism for Electro-Reductive Dioxygen Activation and the Raman Bands of Each Detected Species]**

A 2015 study reported an electro-reductive activation strategy utilizing the non-heme complex  $[\text{Fe}^{\text{II}}(\text{TPEN})]^{2+}$  as a precursor. The pertinent intermediates— $[\text{Fe}^{\text{III}}(\text{OO})(\text{TPEN})]^+$ ,  $[\text{Fe}^{\text{III}}(\text{OOH})(\text{TPEN})]^{2+}$ , and  $[\text{Fe}^{\text{IV}}(\text{O})(\text{TPEN})]^{2+}$ —were chemically synthesized in high yield and characterized via electrochemical techniques [59]. The interaction of  $[\text{Fe}^{\text{II}}(\text{TPEN})]^{2+}$  with  $\text{O}_2$  was investigated using cyclic voltammetry. Analysis and simulation of the data indicated that the iron(III) peroxy complex,  $[\text{Fe}^{\text{III}}(\text{OO})(\text{TPEN})]^+$ , forms via one-electron reduction of a rarely observed  $\text{Fe}^{\text{II}}\text{-O}_2$  adduct at  $-0.62\text{ V}$  versus SCE [59]. This occurs at a significantly more positive potential than the reduction of free dioxygen to superoxide, which was measured at  $-0.87\text{ V}$ . Crucially, and in distinction to other systems, the electrochemical results showed no indication of  $\text{O-O}$  bond cleavage for the  $[\text{Fe}^{\text{III}}(\text{OO})(\text{TPEN})]^+$  species within the experimental timeframe and conditions of the study (Figure 19).

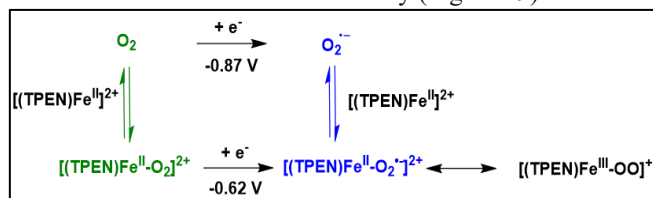


**[Fig.19 : Proposed Reductive Activation Mechanism of O2 at  $[\text{Fe}^{\text{II}}(\text{TPEN})]^{2+}$  Based on Modelisation of Experimental CVs]**

An alternative route for dioxygen activation employs a synthetic catalyst-mediated autooxidation process. This method is particularly advantageous because it does not require an external electron donor. The mechanism, first delineated in the 1980s, involves the initial generation of a  $\mu$ -

peroxy diiron(III) species, followed by homolytic  $\text{O-O}$  bond cleavage to yield an iron(IV)-oxo intermediate [60]. This  $\mu$ -peroxy diiron(III) porphyrin intermediate was successfully isolated and characterized, with investigations using  $^1\text{H NMR}$  and UV-visible spectroscopy verifying its gradual conversion to the iron(IV)-oxo species at low temperatures (between  $-80$  and  $-30\text{ }^\circ\text{C}$ ). When 50 equivalents of triphenylphosphine ( $\text{PPh}_3$ ) are introduced,  $\text{Fe}^{\text{II}}\text{TPP}$  can catalyze oxygen atom transfer to produce  $\text{O=PPh}_3$ , attaining a turnover number (TON) of 27 before catalyst deactivation. This deactivation is associated with the formation of an inactive  $\mu$ -oxo diiron(III) porphyrin species, which was identified in solution upon reaction completion (Figure 20).

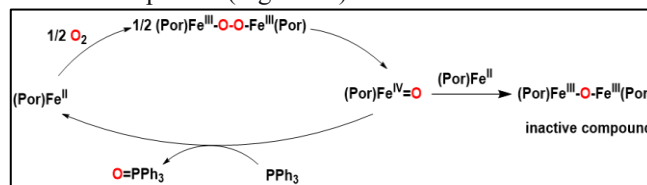


**[Fig.20: Proposed Mechanism for Dioxygen Activation by Iron Porphyrin Complex]**

Significantly, the inactive  $\mu$ -oxo diiron(III) porphyrin complex can be reactivated photochemically. Irradiation with visible light induces homolytic cleavage of the  $\text{Fe-O-Fe}$  bridge, producing an iron(II) porphyrin and a reactive iron(IV)-oxo species capable of oxygenating diverse substrates. Research has demonstrated that this  $\mu$ -oxo diiron(III) Pacman porphyrin serves as an effective catalyst for the photo-driven oxidation of sulfides, alkenes, and alkanes in non-coordinating solvents such as benzene and toluene. A  $\mu$ -oxo diiron(III) Pacman porphyrin exhibited substantially greater reactivity compared to its non-bridged counterpart, an enhancement ascribed to its binuclear architecture, which promotes dioxygen coordination across the two iron centres and facilitates  $\mu$ -peroxy bond formation. However, the precise mechanism for the initial formation of the  $\mu$ -oxo diiron(III) Pacman porphyrin from dioxygen and its diiron(II) precursor remains an area for further elucidation (Figure 21).

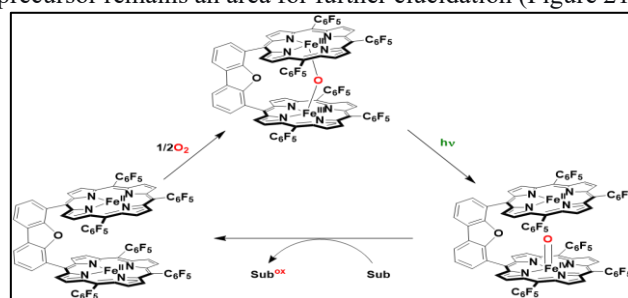


**[Fig.21: Photocycle of the Catalytic Oxidation of Substrates by  $\mu$ -oxo Diiron(III) Pacman Porphyrin Using Dioxygen Without Need for an External Coreductant]**

The non-heme complex  $[\text{Fe}^{\text{II}}(\text{TMC})(\text{OTf})_2]$  can activate dioxygen, likely through a  $\mu$ -peroxy diiron(III) intermediate, although its catalytic performance is relatively low. It achieves turnover numbers (TONs) of 8 for the oxidation of triphenylphosphine ( $\text{PPh}_3$ ) to  $\text{O=PPh}_3$ , 7 for the conversion of thioanisole to methyl phenyl sulfoxide, and 6 for the transformation of benzyl





alcohol to benzaldehyde. This constrained activity may partially result from catalyst deactivation via the formation of an undetected  $\mu$ -oxo diiron(III) species. Moreover, investigations indicate that the electron-rich character of these iron(II) complexes—reflected in their low  $\text{Fe}^{\text{III}}/\text{Fe}^{\text{II}}$  redox potentials ( $< -0.1$  V vs  $\text{Fc}^+/\text{Fc}$ )—is essential for dioxygen activation to produce iron(IV)-oxo species. This accounts for why other non-heme complexes such as  $[\text{Fe}^{\text{II}}(\text{TPA})]^{2+}$ ,  $[\text{Fe}^{\text{II}}(\text{N4Py})]^{2+}$ , and  $[\text{Fe}^{\text{II}}(\text{BPMEN})]^{2+}$  do not generate iron(IV)-oxo intermediates from  $\text{O}_2$ .

In a distinct system, the  $\mu$ -oxo diiron(IV) 1-TAML complex, first characterized by Collins and colleagues in 2004, is also capable of oxygenating substrates. Its formation from the iron(III) 1-TAML precursor and  $\text{O}_2$  is proposed to proceed through  $\mu$ -peroxo diiron(IV) and iron(V)-oxo intermediates, analogous to the pathway suggested for  $\mu$ -oxo diiron(III) species. The pronounced reactivity of the iron(III) complex with dioxygen is ascribed to its four strongly electron-donating amidato nitrogen ligands, which provide exceptional stabilization to the metal center in high oxidation states. The structure of this  $\mu$ -oxo diiron(IV) species has been confirmed by X-ray crystallography. In catalytic oxidations, this complex is thought to function as a precursor, decomposing in the presence of substrates to generate an iron(V)-oxo species identified as the active oxidant. Therefore, the  $\mu$ -oxo diiron(IV) 1-TAML complex acts as an effective catalyst for oxidizing a range of substrates using dioxygen as the terminal oxidant (Figure 22).

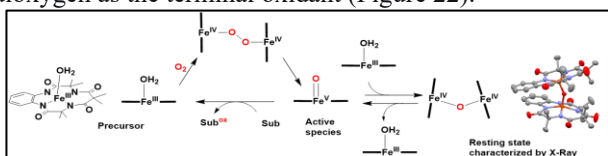


**[Fig.22: Proposed Mechanism for the Oxygenation of Substrates by Dioxygen Catalyzed by Iron(III) TAML Complex in the Presence of  $\text{O}_2$ ]**

Additional photocatalytic strategies have been devised that employ a light-absorbing chromophore paired with an electron donor to facilitate the photoinduced activation of  $\text{O}_2$  at an iron catalyst centre.

iii. Using Water as an Oxygen Source

Like dioxygen, water is an environmentally benign oxygen source and is integral to the generation of manganese(V)-oxo intermediates in the natural water-splitting cycle of Photosystem II (PSII). This enzymatic complex catalyzes the oxidation of water to molecular oxygen alongside the reduction of plastoquinone. Detailed studies of its oxygen-evolving complex (OEC) suggest that the crucial  $\text{Mn}^{\text{V}}=\text{O}$  species forms through a proton-coupled electron transfer (PCET) mechanism, involving the two-electron oxidation of a water molecule bound within the manganese cluster. In this biological system, the absorption of visible light by chlorophyll initiates a series of PCET steps that ultimately oxidize a manganese-bound water molecule to yield the high-valent manganese-oxo intermediate (Figure 23).

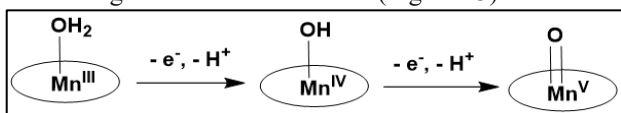


**[Fig.23: Formation of  $\text{Mn}^{\text{V}}=\text{O}$  Species in PCET Mechanism Using Water as an Oxygen Source]**

Researchers have engineered numerous synthetic metal complexes, including iron-based systems, to generate high-valent metal-oxo species using water as the oxygen atom donor. A pioneering accomplishment in 2009 was the first reported synthesis of a synthetic iron-oxo complex,  $[\text{Fe}^{\text{IV}}=\text{O}(\text{N4Py})]^{2+}$ , from its precursor  $[\text{Fe}^{\text{II}}(\text{H}_2\text{O})(\text{N4Py})]^{2+}$ . This conversion utilized water as the oxygen source and cerium(IV) as a powerful one-electron oxidant. The resulting species catalyses the oxygenation of substrates such as thioanisole, benzyl alcohol, cyclohexene, and ethylbenzene. Expanding on this, a follow-up study developed a photocatalytic system that also produced the active  $[\text{Fe}^{\text{IV}}=\text{O}(\text{N4Py})]^{2+}$  species. This system employed the same iron catalyst, a  $[\text{Ru}(\text{bpy})_3]^{3+}$  photosensitizer, and  $[\text{Co}^{\text{III}}(\text{NH}_3)_5]\text{Cl}$  as a sacrificial electron acceptor. This work confirmed that the potent iron-oxo intermediate could be formed using the milder oxidant  $[\text{Co}^{\text{III}}(\text{NH}_3)_5]\text{Cl}$  in a light-driven process with water (Figure 24).

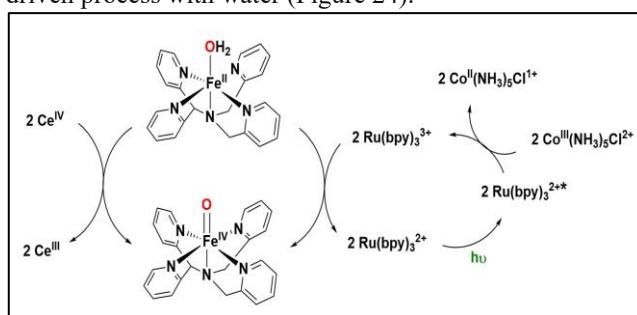


**[Fig.24: Formation of  $[\text{Fe}^{\text{IV}}=\text{O}(\text{N4Py})]^{2+}$  by Water Chemical Activation Using Cerium(IV) (left) as an Oxidant or by Water Photoactivation Using a Chromophore and a Sacrificial Electron Donor (Right)]**

The high-valent iron(V)-oxo complex  $[\text{Fe}^{\text{V}}=\text{O}(\text{TAML})]^{1-}$  has been prepared by oxidizing its iron(III)-aqua precursor,  $[\text{Fe}^{\text{III}}(\text{OH}_2)(\text{TAML})]^{1-}$ . This can be accomplished chemically using a potent oxidant such as cerium(IV) or photochemically with  $[\text{Ru}(\text{bpy})_3]^{2+}$  as a photosensitizer and sodium dithionite as a sacrificial electron donor. Another electrochemical method involves activating the metal-bound water molecule. Stahl and colleagues demonstrated this approach by electrochemically oxidizing  $[\text{Fe}^{\text{III}}(\text{OH}_2)(1\text{-TAML})]^{1-}$ , successively generating the  $[\text{Fe}^{\text{IV}}(\text{OH})(1\text{-TAML})]^{1-}$  and  $[\text{Fe}^{\text{V}}=\text{O}(1\text{-TAML})]^{1-}$  species at applied potentials of 0.34 V and 0.79 V versus  $\text{Fc}^+/\text{Fc}$ , respectively. These electrogenerated species were subsequently employed to catalyze the oxidation of organic substrates, including alkylbenzenes and benzyl alcohol [59].

In a related strategy, several iron(IV)-oxo complexes supported by non-heme polynitrogen ligands were generated quantitatively via bulk electrolysis in acetonitrile, using water (0.1–1 M) as the oxygen source. Cyclic voltammetry of the iron(II) precursors in dry acetonitrile displayed only a  $\text{Fe}^{\text{III}}(\text{CH}_3\text{CN})/\text{Fe}^{\text{II}}(\text{CH}_3\text{CN})$  redox couple. Upon the addition of water, a new reduction wave emerged at a more negative potential, signifying ligand exchange where acetonitrile is replaced by water to form an  $\text{Fe}^{\text{II}}(\text{OH}_2)(\text{L})$  complex. The iron(II)-aqua species undergoes a two-step, one-electron oxidation, with each step accompanied by deprotonation at a distinct



## Sustainable Catalysis and Biomedical Applications: Advancing Iron-Based Oxygen Atom Transfer Through Bioinspired Ligand Design

potential. For instance,  $[\text{Fe}^{\text{II}}(\text{H}_2\text{O})(\text{N4Py})]^{2+}$  is initially oxidized to  $[\text{Fe}^{\text{III}}(\text{OH})(\text{N4Py})]^{2+}$  at 0.6 V versus  $\text{Fc}^+/\text{Fc}$ , and subsequently to  $[\text{Fe}^{\text{IV}}=\text{O}(\text{N4Py})]^{2+}$  at 0.9 V [58]. The potential of the  $\text{Fe}^{\text{IV}}=\text{O}/\text{Fe}^{\text{III}}-\text{OH}$  redox couple serves as an indicator of its oxidizing strength. Research by Comba, Costas, and Que has established a direct relationship: a higher potential for this couple correlates with increased reactivity of the  $\text{Fe}^{\text{IV}}=\text{O}$  species in oxygenating substrates such as thioanisole, benzyl alcohol, and 1,3-cyclohexadiene [59].

### iv. Quest for the Active Iron Species

High-valent iron-oxo intermediates have been a central focus of research for many years, motivated by the dual aims of elucidating enzymatic mechanisms and developing efficient, sustainable catalysts for oxidation reactions such as alkene epoxidation and alkane hydroxylation. An array of spectroscopic techniques is utilized to characterize these often short-lived species, including absorption, Mössbauer, electron paramagnetic resonance (EPR), Raman, and nuclear magnetic resonance (NMR) spectroscopy, as well as mass spectrometry (MS).

Mössbauer and EPR spectroscopies are especially critical for establishing the oxidation state of the iron and its ligand field geometry. Resonance Raman spectroscopy serves as the principal method for investigating the vibrational energy of the  $\text{Fe}=\text{O}$  bond. Although mass spectrometry can provide structural information, X-ray diffraction yields unambiguous atomic-resolution structural data. A major obstacle, however, is the inherent instability of these reactive iron-oxo species, which often precludes their crystallization even at low temperatures. In such instances, extended X-ray absorption fine structure (EXAFS) analysis is an essential tool, providing insights into the iron centre's oxidation state and its local coordination environment, including  $\text{Fe}-\text{O}$  bond distances (Figure 25).

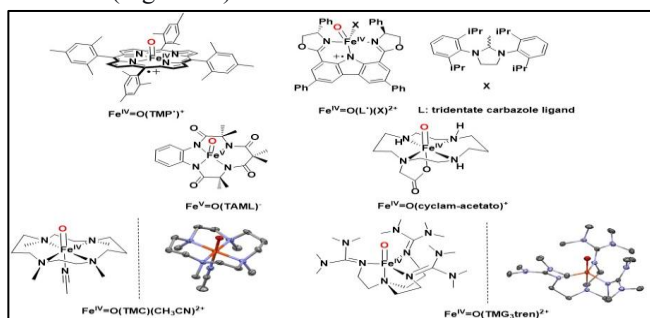


**[Fig.25: Structure of Selected Iron-oxo Species with the ORTEP Plot of Their X-Ray Diffraction Analysis When Performed]**

The iron(IV)-oxo porphyrin  $\pi$ -cation radical complex  $[\text{Fe}^{\text{IV}}=\text{O}(\text{TMP}^{\bullet+})]^{+}$ , a synthetic analogue of cytochrome P-450's Compound I, was first isolated and characterized in 1981. It was prepared by oxidizing  $[\text{Fe}^{\text{III}}(\text{TMP})\text{Cl}]$  with *meta*-chloroperoxybenzoic acid (\*m\*CPBA) at  $-78\text{ }^{\circ}\text{C}$ . Its assignment as a Compound I mimic was confirmed by UV-

visible spectroscopy, exhibiting a broad Soret band at 406 nm and a Q-band at 645 nm. Mössbauer and EPR spectroscopies revealed ferromagnetic coupling between the  $S=1$   $\text{Fe}^{\text{IV}}$  centre and the porphyrin radical ( $S=1/2$ ), with EPR signals at  $g = 4.3, 3.9, \text{ and } 2.0$ . EXAFS analysis indicated a short  $\text{Fe}=\text{O}$  bond length of 1.6 Å, consistent with a double bond, a finding corroborated by a resonance Raman vibration at  $828\text{ cm}^{-1}$ . Following this initial work, numerous related iron(IV)-oxo porphyrin cation radical complexes with modified macrocycles have been synthesized and characterized, enabling the establishment of structure-activity relationships [60].

Beyond heme systems, a non-heme iron(III) complex bearing a tridentate carbazole ligand was shown to generate an iron(IV)-oxo ligand cation radical upon reaction with the two-electron oxidant PhIO. This species, capable of alkene epoxidation, highlights the role of a  $\pi$ -conjugated ligand framework in stabilizing radical character. Its identification was based on a characteristic absorption band at 660 nm and an EPR signal at  $g = 2.0$ , ascribed to a ligand-centred radical. Importantly, the lack of observable coupling between the iron centre and the radical, in contrast to porphyrin systems, suggests a distinct electronic structure that requires further investigation.

The first non-heme iron(IV)-oxo species was reported in 2000, generated via ozonolysis of an iron(III) precursor at  $-80\text{ }^{\circ}\text{C}$ . While this intermediate exhibited limited stability, the subsequent use of the stronger-field TMC ligand enabled the synthesis of  $[\text{Fe}^{\text{IV}}=\text{O}(\text{TMC})(\text{CH}_3\text{CN})]^{2+}$ , a species stable for weeks at  $-40\text{ }^{\circ}\text{C}$ . This durability enabled comprehensive characterisation, including X-ray crystallography, which revealed a  $\text{Fe}=\text{O}$  bond length of 1.64 Å, similar to that observed for the ferrate ion ( $\text{FeVIO}_4^{2-}$ ).

The substantially higher reactivity of iron(V)-oxo species has rendered their isolation considerably more difficult. Their formation is often deduced from the decay of a proposed  $\text{Fe}^{\text{V}}=\text{O}$  precursor to a  $\text{Fe}^{\text{IV}}=\text{O}$  species, an inference supported by the high redox potential of the  $\text{Fe}^{\text{V}}=\text{O}/\text{Fe}^{\text{IV}}-\text{OH}$  couple. Most characterized  $\text{Fe}^{\text{V}}=\text{O}$  species are stable only at cryogenic temperatures. A landmark accomplishment was Collins' 2007 report of  $[\text{Fe}^{\text{V}}=\text{O}(1\text{-TAML})]^{-}$ , stabilized by the strongly electron-donating TAML ligand. Its +5 oxidation state was verified by a distinctive negative Mössbauer isomer shift ( $\delta = -0.46\text{ mm/s}$ ), an EPR signature consistent with a low-spin ( $S = 1/2$ ) configuration, and an extremely short  $\text{Fe}-\text{O}$  bond (1.58 Å) from EXAFS data. To date, no high-spin ( $S = 3/2$ ) iron(V)-oxo species have been characterized, likely because the strong ligand fields necessary to access the +5 oxidation state enforce a low-spin configuration. The extreme reactivity of these species has also prevented the determination of a crystal structure (Table 3).



Table III: Spectroscopic Characterizations of Fe<sup>V</sup>=O Species

Proposed formulation	$\lambda_{\text{max}}$ (nm) ( $\epsilon$ ) ( $\text{M}^{-1}\cdot\text{cm}^{-1}$ )	EPR g values	Mössbauer $\delta$ ( $\text{mm}\cdot\text{s}^{-1}$ )	Raman $\nu$ (Fe-O) ( $\text{cm}^{-1}$ )	Fe-O bond ( $\text{\AA}$ )
Fe <sup>V</sup> =O(1-TAML)	445 (5400) 630 (4200)	1.99, 1.97, 1.74	-0.42	-	1.58
Fe <sup>V</sup> =O(b-TAML)	441 (4350) 613 (3420)	1.98, 1.94, 1.73	-0.44	-	-
Fe <sup>V</sup> =O(TPA)	-	2.71, 2.42, 1.53	-	-	-
Fe <sup>V</sup> =O(BPMEN)	-	2.69, 2.42, 1.70	-	-	-
Fe <sup>V</sup> =O(PDP)	-	2.66, 2.42, 1.71	-	-	-
Fe <sup>V</sup> =O(PyTACN)	-	2.66, 2.43, 1.74	-	-	-
Fe <sup>V</sup> =O(PyNMe <sub>3</sub> )	490	2.07, 2.01, 1.95	-	-	-
Fe <sup>V</sup> =O(TMC)(NCOCH <sub>3</sub> )	410 (4000) 780 (430)	2.05, 2.01, 1.97	0.1	798	-

Interestingly, efforts to isolate well-defined Fe=O species have led to the identification of transient iron-oxo adducts, formulated as FeO-X (where X = Cl, OH, O, or OAc). These intermediates are now recognized as precursors that can undergo further transformation to yield the terminal Fe=O unit. In several instances, these FeO-X species have themselves been characterized as the direct oxidants responsible for substrate oxygenation.

#### IV. CONCLUSION

The advancement of bioinspired iron complexes for oxygen atom transfer (OAT) constitutes significant progress toward sustainable catalytic technologies. This research highlights the potential of synthetic iron-based systems to mirror the efficacy of natural metalloenzymes, enabling efficient and selective oxidations under ambient conditions. Guided by biological blueprints, we have developed catalysts that not only facilitate OAT but also display enhanced stability and activity.

Our investigation of novel dipyrin-based iron complexes has been particularly revealing, demonstrating their proficiency in stabilizing the high-valent iron-oxo intermediates essential to OAT chemistry. Comprehensive spectroscopic studies have been critical for elucidating the electronic structure of these reactive species, yielding pivotal insights that expand our fundamental understanding of iron-catalysed oxidation mechanisms. A central achievement of this work is the effective utilization of environmentally benign oxidants—dioxygen and water—in alignment with the principles of green chemistry. We have established that our complexes can activate these abundant resources to generate reactive iron-oxo species, thereby offering a route to diminish the ecological impact of oxidation processes.

The bioinspired design strategy has also provided a clearer view of the detailed mechanics governing OAT. By clarifying how substrates interact with the iron centre, we are better positioned to engineer ligand frameworks that optimise catalytic performance. The deliberate incorporation of electron-donating and sterically tailored ligands has effectively increased the electrophilicity, and consequently the oxidative strength, of the iron-oxo core. A persistent obstacle in this area is the intrinsic lability of high-valent iron intermediates. We have addressed this by employing innovative activation methods that use mild reductants and refined conditions to generate and utilise these transient species within productive catalytic cycles.

Prospectively, the insights derived from this work establish a strong foundation for the continued development of iron-

based catalysis. Future endeavours will focus on expanding the substrate range of these oxidations and evaluating their potential for industrial application. Ongoing mechanistic inquiry will be essential to resolve remaining complexities in iron-mediated OAT, thereby informing the design of next-generation catalysts with superior efficiency and selectivity.

Bioinspired iron complexes represent a highly promising direction in catalysis, effectively connecting biological inspiration with synthetic innovation. By deepening our comprehension of these systems, we advance toward the broader goal of establishing sustainable and potent catalytic technologies that meet the demands of modern chemical synthesis while maintaining environmental stewardship. This research not only enriches the fundamental science of iron-mediated reactions but also provides a conceptual framework for future advancements in the field.

#### DECLARATION STATEMENT

Some of the references cited are older and are noted explicitly as [1], [2], [3], [4], [5], [6], [7], and [13]. However, these works remain significant for the current study, as they are pioneering in their fields.

After aggregating input from all authors, I must verify the accuracy of the following information as the article's author.

- **Conflicts of Interest/ Competing Interests:** Based on my understanding, this article has no conflicts of interest.
- **Funding Support:** This article has not been funded by any organizations or agencies. This independence ensures that the research is conducted objectively and free from external influence.
- **Ethical Approval and Consent to Participate:** The content of this article does not necessitate ethical approval or consent to participate with supporting documentation.
- **Data Access Statement and Material Availability:** The adequate resources of this article are publicly accessible.
- **Author's Contributions:** The authorship of this article is contributed equally to all participating individuals.

#### REFERENCES

1. Machkour A, Thallaj NK, Benhamou L, Lachkar M, Mandon D. *Chemistry*. 2006 Aug 25;12(25): 6660-8.



# Sustainable Catalysis and Biomedical Applications: Advancing Iron-Based Oxygen Atom Transfer Through Bioinspired Ligand Design

- DOI: <https://doi.org/10.1002/chem.200600276>. The works remain significant, see the [declaration](#)
- Thallaj, N., Machkour, A., Mandon, D., Welter, R., New. J. Chem., 2005, 29, 1555 – 1558.  
DOI: <https://doi.org/10.1039/B512108F>, works remain significant, see the [declaration](#)
  - Thallaj NK, Rotthaus O, Benhamou L, Humbert N, Elhabiri M, Lachkar M, Welter R, Albrecht-Gary AM, Mandon D. Chemistry–A European Journal 14 (22), 6742–6753. 2008.  
DOI: <https://doi.org/10.1002/chem.200701967>, works remain significant, see the [declaration](#)
  - Wane A, Thallaj NK, Mandon D. Chemistry. 2009 Oct 12;15(40):10593–602. P10594–10595–10595.  
DOI: <https://doi.org/10.1002/chem.200901350>, works remain significant, see the [declaration](#)
  - Thallaj NK, Orain PY, Thibon A, Sandroni M, Welter R, Mandon D. Inorg Chem. 2014 Aug 4;53(15):7824–36. P7826–7828.  
DOI: <https://doi.org/10.1021/ic500096h>, works remain significant, see the [declaration](#)
  - N. K. Thallaj, J. Przybilla, R. Welter and D. Mandon, J. Am. Chem. Soc. 2008, 130, 2414–2415.  
DOI: <https://doi.org/10.1021/ja710560g>, works remain significant, see the [declaration](#)
  - N. K. Thallaj, D. Mandon and K. A. White, Eur. J. of Inorg. Chem., 2007, 44–47.  
DOI: <https://doi.org/10.1002/ejic.200600789>. Works remain significant, see the [declaration](#)
  - Thallaj, N. Review of a Few Selected Examples of Intermolecular Dioxigenases Involving Molecular Oxygen and Non-Heme Iron Proteins. Int. J. Adv. Pharmacol. Sci. Res. (IJAPSR) (2023), 3, 1–18.  
DOI: <https://doi.org/10.54105/ijapsr.C4011.023223>
  - L. Labban, M. Kudsi, Z. Malek, N. Thallaj; Advances in Medical, Dental and Health Sciences, 2020,3, 3,45–48.  
DOI: <https://doi.org/10.5530/amdhs.2020.3.11>
  - L. Labban, N. Thallaj, M. Al Masri; Journal of Advanced Research in Food Science and Nutrition, 2020,3,1,34–41.  
DOI: <https://doi.org/10.11648/j.wjfst.20190304.11>  
<http://www.florajournal.com>
  - L. labban; N. thallaj; A. labban; archives of medicine, 2020, 12, 2:8, 1–5. DOI: <https://doi.org/10.36648/1989-5216.12.2.309>
  - L. Labban, N. Thallaj, Z. Malek; Journal of Medical Research and Health Sciences, 2019, 2, 11, 784–787.  
DOI: <https://doi.org/10.15520/jmrhs.v2i11.128>
  - Malek, Z.S.; Dardente, H.; Pevet, P.; Raison, S.; European Journal of Neuroscience 2005, 22 (4), 895–901.  
DOI: <https://doi.org/10.1111/j.1460-9568.2005.04264.x> Works remain significant, see the [declaration](#)
  - A. Abbood, S.A. Malik, D. aldiab, H. H.Ali, N.Thallaj. Investigation of the charge variant profile of non-cleavable conjugated antibodies, Research J. Pharm. and Tech. 2025; 18(1) 185–190.  
DOI: <https://doi.org/10.52711/0974-360X.2025.00028>
  - Malek, Z.S.; Labban, L.; The International Journal of Neuroscience, 2020, 1–7. DOI: <https://doi.org/10.1080/00207454.2020.1782903>
  - ZS Malek, LM Labban; Journal of current research in physiology and pharmacology, 2020, 4, (1),1–5.  
DOI: <https://doi.org/10.31878/IJCRPP.2020.41.01>
  - L.M. Labban, M. M. Alshishkli, A. Alkhalaf, Z. Malek; J. Adv. Res. Dent. Oral Health, 2017, 2(3&4), 1–4.  
DOI: <https://doi.org/10.24321/2456.141X.201702>.
  - L Labban, ZS Malek, Open Access Library Journal, 2018, 5 (07), 1–11.  
DOI: <https://doi.org/10.4236/oalib.1104654>.
  - Y. alhomush, Z. malek, A. Abboud, N.Thallaj, Research Journal of Pharmacy and Technology, 2022, 15, 10.  
DOI: <https://doi.org/10.52711/0974-360X.2022.00794>
  - A.Abboud, Z.Malek, N.Thallaj. 2022 15, 11, 4935–4939. Research Journal of Pharmacy and Technology.  
DOI: <https://doi.org/10.52711/0974-360X.2022.00829>
  - Thallaj, N; agha, M. I ,H., nattouf; A.H; katib, CH; karaali, A; Moustapha, A; Labban L;open access library journal, 2020,7,5,1–21.  
DOI: <https://doi.org/10.4236/oalib.1106302>.
  - N.Thallaj.Xi'an ShiyouDaxueXuebao (ZiranKexue Ban)/ Journal of Xi'an Shiyou University, Natural Sciences Edition.2022.65, 06. 289–301. DOI: <https://doi.org/10.17605/OSF.IO/W8RSS>
  - N.Thallaj. Xi'an ShiyouDaxueXuebao (ZiranKexue Ban)/ Journal of Xi'an Shiyou University, Natural Sciences Edition.2022.65, 06. 313–328. DOI: <https://doi.org/10.17605/OSF.IO/K8RFE>
  - Z. MALEK, A. ABOOD, N.THALLAJ. Xi'an ShiyouDaxueXuebao (ZiranKexue Ban) Journal of Xi'an Shiyou University, Natural Sciences Edition.2022.65, 06. 302–312.  
DOI: <https://doi.org/10.17605/OSF.IO/K56XY>
  - N.Thallaj. 2022. 65, 7, 169–184. Xi'an Shiyou Daxue Xuebao (Ziran Kexue Ban)/Journal of Xi'an Shiyou University, Natural Sciences Edition. DOI: <https://doi.org/10.17605/OSF.IO/7F23D>
  - Z. MALEK,2022. 65, 7, 143–152. Xi'an Shiyou Daxue Xuebao (Ziran Kexue Ban)/Journal of Xi'an Shiyou University, Natural Sciences Edition. DOI: <https://doi.org/10.17605/OSF.IO/2UNHK>
  - N.Thallaj. 2022. 65, 7, 110–142. Xi'an Shiyou Daxue Xuebao (Ziran Kexue Ban)/Journal of Xi'an Shiyou University, Natural Sciences Edition. DOI: <https://doi.org/10.17605/OSF.IO/KZRJD>
  - N.Thallaj. International Journal of Advanced Pharmaceutical Sciences and Research (IJAPSR) 2022. 2, 3,1–28.  
DOI: <https://doi.org/10.54105/ijapsr.C4018.042322>
  - N.Thallaj. International Journal of Advanced Pharmaceutical Sciences and Research (IJAPSR) 2022. 2, 4,1–15.  
DOI: <https://doi.org/10.54105/ijapsr.C4016.062422>
  - N.Thallaj. International Journal of Advanced Pharmaceutical Sciences and Research (IJAPSR) 2022. 2, 6,1–12.  
DOI: <https://doi.org/10.54105/ijapsr.C4015.102622>
  - N.Thallaj. International Journal of Advanced Pharmaceutical Sciences and Research (IJAPSR) 2023. 3, 3,1–10.  
DOI: <https://doi.org/10.54105/ijapsr.C4012.043323>
  - N.Thallaj. International Journal of Advanced Pharmaceutical Sciences and Research (IJAPSR) 2024. 4, 1,32–52.  
DOI: <https://doi.org/10.54105/ijapsr.A4036.124123>
  - N.Thallaj. International Journal of Advanced Pharmaceutical Sciences and Research (IJAPSR) 2024. 4, 5,29–49.  
DOI: <https://doi.org/10.54105/ijapsr.E4049.04050824>.
  - N.Thallaj. International Journal of Advanced Pharmaceutical Sciences and Research (IJAPSR) 2024.4, 4,7–21.  
DOI: <https://doi.org/10.54105/ijapsr.D4042.04040624>
  - N.Thallaj. International Journal of Advanced Pharmaceutical Sciences and Research (IJAPSR) 2024.4, 6,7–27.  
DOI: <https://doi.org/10.54105/ijapsr.F4054.04061024>
  - N.Thallaj. International Journal of Advanced Pharmaceutical Sciences and Research (IJAPSR) 2024.4, 6,33–48.  
DOI: <https://doi.org/10.54105/ijapsr.F4055.04061024>
  - Thallaj, N. (2024). Advancements in Pharmaceutical Science: Synthesis and Application of Molecular Cages Integrating N-Heterocyclic Carbenes for Enhanced Stability and Functionality. International Journal of Advanced Pharmaceutical Sciences and Research (IJAPSR), 5(1), 6–19.  
DOI: <https://doi.org/10.54105/ijapsr.A4063.05011224>
  - Ayat Abbood, Hassan Hadi Ali, Samir Azzat Malik, Dima AlDiab, Nasser Thallaj. Investigation of the Charge Variant Profile of Non-cleavable Conjugated Antibodies. Research Journal of Pharmacy and Technology. 2025;18(1):185–0.  
DOI: <https://doi.org/10.52711/0974-360X.2025.00028>
  - Thallaj, N. Analyzing Charge Variant Profiles of Monoclonal Antibodies Conjugated to Cytotoxic Agents. International Journal of Advanced Pharmaceutical Sciences and Research (IJAPSR), Volume-4 Issue-3, April 2025, pages 20–26.  
DOI: <https://doi.org/10.54105/ijapsr.C4071.05030425>.
  - Thallaj, N. Biomimetic Synthesis and Phytochemical Analysis of Lodopyridone: Insights into 4-Pyridone Derivatives and Thiopeptide Antibiotic. Journal of Advanced Pharmaceutical Sciences and Research (IJAPSR), Volume-4 Issue-3, April 2025, pages 9–19.  
DOI: <https://doi.org/10.54105/ijapsr.B4069.05030425>
  - Mousa Al Khleif, Nour Alhuda Alzoubi, Ghassan Shannan, Zeina S Malek, Nasser Thallaj\*. Exploring Circadian Rhythms: A Comprehensive Study on Sleep Patterns and Disorders in Syrian Society. Am J Biomed Sci & Res. 2025 26(2) AJBSR.MS.ID.003416, DOI: <https://doi.org/10.34297/AJBSR.2025.26.003416>.
  - Ranim Abdul Rahman, Louai Alallan, Ahmed Khalid Aldhalmi, Nasser Thallaj. Separation, Determination, and Potential Application of Active Compounds in Porosopis cineraria: A Comprehensive Analysis. Research Journal of Pharmacy and Technology. 2025;18(4):1604–0. DOI: <https://doi.org/10.52711/0974-360X.2025.00230>
  - Dalia Aboufakher, Rita Zeinaldin, Racha Khatib, Rawa Khreit, Mohamed Sami Joha, Nasser Thallaj. Prevalence and Antibiotic Resistance Patterns of Multidrug-Resistant Gram-Negative Bacilli in Hospitalized Patients in Sweida, Syria. Am J Biomed Sci & Res. 2025 26(3) AJBSR.MS.ID.003436,



- DOI: <https://doi.org/10.34297/AJBSR.2025.26.003436>.
44. Beshar S, Alallan L, Hasan Agha MI, Alshamaa I, Thallaj N. Influence of Soil Salinity on the Chemical Composition of Essential Oil of *Rosmarinus officinalis* in Syria. *Research Journal of Pharmacy and Technology*. 2024; 17(5):2282- 8.  
DOI: <https://doi.org/10.52711/0974-360X.2024.00358>.
45. Khatib O, Alshimale T, Alsaadi A Thallaj N. The Global Impact of HIV: A Comprehensive Review. *IJAPSR*, vol. 4, no. 3, pp. 6–19, Apr. 2024.  
DOI: <https://doi.org/10.54105/ijapsr.C4040.04030424>.
46. Samer Alkhoury, Rasha Kateeb, Rawa Akasha and Nasser Thallaj\*. Analysis of Crocin Content in Saffron (*Crocus sativus* L) Cultivated in Syria Using Liquid Chromatography-Mass Spectrometry. *Am J Biomed Sci & Res*. 2025 26(3) AJBSR.MS.ID.003443,  
DOI: <https://doi.org/10.34297/AJBSR.2025.26.003443>.
47. Thallaj, N. (2022). Design and Synthesis Ligands Tetrads Substituted with Halogenes in  $\alpha$ - Position and Conjugation with Riboflavin (Bioconjugates): Conjugate ligands Type TPA's with Flavonoids as an Electron Mediator. *Biomedicine and Chemical Sciences*, 1(2), 47–56,  
DOI: <https://doi.org/https://doi.org/10.48112/bcs.v1i2.85>.
48. Thallaj, N., Alrasho, J. F., & Sofi, F. K. (2024). Advancements in Antiviral Therapeutics: A Comprehensive Review of Hepatitis C Virus and Novel Flavone Leads. *International Journal of Advanced Pharmaceutical Sciences and Research (IJAPSR)*, 5(1), 28-40.  
DOI: <https://doi.org/10.54105/ijapsr.A4064.05011224>.
49. Thallaj, N. Analyzing Charge Variant Profiles of Monoclonal Antibodies Conjugated to Cytotoxic Agents. *International Journal of Advanced Pharmaceutical Sciences and Research (IJAPSR)*, Volume-5 Issue-3, April 2025, pages 20-26.  
DOI: <https://doi.org/10.54105/ijapsr.C4071.05030425>.
50. Thallaj, N. Biomimetic Synthesis and Phytochemical Analysis of Lodopyridone: Insights into 4-Pyridone Derivatives and Thiopeptide Antibiotics. *International Journal of Advanced Pharmaceutical Sciences and Research (IJAPSR)*, Volume-5 Issue-3, April 2025, pages 9-19. DOI: <https://doi.org/10.54105/ijapsr.B4069.05030425>.
51. Thallaj, N. (2023). A Brief Overview of the General Characteristics and Reactivity Towards Dioxigen of the Ferrous Tris (2-Pyridylmethyl Amine) Series Complexes is Presented. *International Journal of Advanced Pharmaceutical Sciences and Research (IJAPSR)*, 3(3), 1-18. DOI: <https://doi.org/10.54105/ijapsr.C4012.043323>
52. Thallaj, N. (2024). Advancements in Pharmaceutical Science: Synthesis and Application of Molecular Cages Integrating N-Heterocyclic Carbenes for Enhanced Stability and Functionality. *International Journal of Advanced Pharmaceutical Sciences and Research (IJAPSR)*, 5(1), 6-19.  
DOI: <https://doi.org/10.54105/ijapsr.A4063.05011224>
53. Thallaj, N. (2024). Conductive Nanocomposites Based on Graphene and Natural Polymers. *International Journal of Advanced Pharmaceutical Sciences and Research (IJAPSR)*, 4(6), 7-27  
DOI: <https://doi.org/10.54105/ijapsr.F4054.04061024>
54. Thallaj, N. (2022). Review of Calixarene-Derivatives in Transition Metal Chemistry. *International Journal of Advanced Pharmaceutical Sciences and Research (IJAPSR)*, 2(3), 1-30.  
DOI: <https://doi.org/10.54105/ijapsr.C4018.042322>
55. Thallaj, N. (2024). Advancements in Peptide Vectors for Cancer Therapy and Tumour Imaging: A Comprehensive Review. *International Journal of Advanced Pharmaceutical Sciences and Research (IJAPSR)*, 4(5), 29-49.  
DOI: <https://doi.org/10.54105/ijapsr.E4049.04050824>.
56. Thallaj, N., Ali Hamad, D. H., Batieh, N. A., & Saker, G. A. (2023). A Review of Colon Cancer Treatment Using Photoactive Nanoparticles. *International Journal of Advanced Pharmaceutical Sciences and Research (IJAPSR)*, 3(4), 1-32.  
DOI: <https://doi.org/10.54105/ijapsr.D4022.063423>
57. Shannan, G., Malek, Z. S., & Thallaj, N. (2025). Advancements in Protein Synthesis: Triazole Multi-Ligation and Cycloadditions for Pharmaceutical Applications. *Am J Biomed Sci & Res*, 26(5), 685-700. DOI: <https://doi.org/10.34297/AJBSR.2025.26.003481>
58. E. ARWANI, M. AL SHAREEF, S. HAMZA, Z. MALEK, G. SHANNAN, NASSER THALLAJ Xi'an ShiyouDaxueXuebao (ZiranKexue Ban) / Journal of Xi'an Shiyou University, Natural Sciences Edition.2025.68, 12. 7-24.  
DOI: <https://doi.org/10.5281/zenodo.17894451>
59. NISREEN H. AL. SHIBEH AL. WATTAR, RAWAA KHREIT, RACHA ALKHATIB, NASSER THALLAJ Xi'an ShiyouDaxueXuebao (ZiranKexue Ban) / Journal of Xi'an Shiyou University, Natural Sciences Edition.2025.68, 12. 25-39.  
DOI: <https://doi.org/10.5281/zenodo.17894613>.

60. Zeina S Malek, Ghassan Channan, Nasser Thallaj, Xi'an ShiyouDaxueXuebao (ZiranKexue Ban) / Journal of Xi'an Shiyou University, Natural Sciences Edition.2025.68, 10. 1-35.  
DOI: <https://doi.org/10.5281/zenodo.17321958>.

## AUTHOR'S PROFILE



**Prof. Dr Ghassan Shannan**, Professor of Clinical Biochemistry and Medical Laboratory Sciences, with academic and professional expertise spanning over five decades in university education, scientific and consultative research, and management and quality of medical laboratories. Currently serving as the Dean of the Faculty of Pharmacy at the Arab International University. Holds a PhD in Clinical Biochemistry from Newcastle upon Tyne University (United Kingdom) and a Bachelor's degree in Pharmacy from Damascus University. Additionally, has received specialized training in several international hospitals and centers in the fields of laboratory medicine, immunoassays, quality assurance, and laboratory management.



**Prof. Dr Zina Malek** is an academic and researcher in neuroscience and physiology. She holds a PhD and a postdoctoral fellowship from Louis Pasteur University in Strasbourg, following a Master's degree in Neurosciences from the same university, where she specialised in demyelinating diseases and neuroimaging. She also earned a Master's degree in Cell Biology and Physiology from the University of Dijon, France, a Postgraduate Diploma in Zoology from Damascus University, and a Bachelor's degree in Biology from the same university.



**Prof. Dr Nasser Thallaj** holds a PhD in Chemical Sciences from Louis Pasteur University – Strasbourg in France, a Master's degree in Transition Metal Chemistry and Molecular Engineering, in addition to a Postgraduate Diploma in Applied Chemistry from the University of Damascus, and a Bachelor's degree in Applied Chemistry from the same university. Following his doctorate, he worked as a researcher in the Laboratory of Nano-Chemistry and Supramolecular Materials at the University of Notre Dame, Belgium, where he focused on drug delivery systems. He then assumed prominent academic and administrative positions at several private Syrian universities.

**Disclaimer/Publisher's Note:** The statements, opinions and data contained in all publications are solely those of the individual author(s) and contributor(s) and not of the Lattice Science Publication (LSP)/ journal and/ or the editor(s). The Lattice Science Publication (LSP)/ journal and/ or the editor(s) disclaim responsibility for any injury to people or property resulting from any ideas, methods, instructions or products referred to in the content.